Eur. Phys. J. A (2016) **52**: 237
DOI 10.1140/epja/i2016-16237-4

THE EUROPEAN PHYSICAL JOURNAL A

Regular Article – Theoretical Physics

Baryon stopping in heavy-ion collisions at $E_{lab} = 2A–200A$ GeV*

Yu.B. Ivanov[1,2,a] and D. Blaschke[2,3,4,b]

[1] National Research Centre "Kurchatov Institute" (NRC "Kurchatov Institute"), 123182 Moscow, Russia
[2] National Research Nuclear University "MEPhI" (Moscow Engineering Physics Institute), 115409 Moscow, Russia
[3] Institute of Theoretical Physics, University of Wroclaw, 50-204 Wroclaw, Poland
[4] Bogoliubov Laboratory of Theoretical Physics, JINR Dubna, 141980 Dubna, Russia

Received: 29 September 2015
Published online: 22 August 2016 – © Società Italiana di Fisica / Springer-Verlag 2016
Communicated by D. Blaschke

Abstract. It is argued that an irregularity in the baryon stopping is a natural consequence of the onset of deconfinement occurring in the compression stage of a nuclear collision. It is an effect of the softest point inherent in an equation of state (EoS) with a deconfinement transition. In order to illustrate this effect, calculations within the three-fluid model were performed with three different EoSs: a purely hadronic EoS, an EoS with a first-order phase transition and a third one with a smooth crossover transition. It is demonstrated that this irregularity is a very robust signal of the first-order phase transition that survives under acceptance conditions of the NICA MPD experiment.

1 Introduction

One of the main goals of the current experiments at RHIC and SPS and forthcoming experiments at FAIR and NICA facilities is to determine a kind of the deconfinement transition in dense baryonic matter and to find the collision energy (thereby the baryonic density) at which this transition starts. In this paper it is argued that the baryon stopping in nuclear collisions can be a sensitive probe of the deconfinement onset. Let us start with discussion in terms of the conventional (*i.e.* one-fluid) hydrodynamics.

The form of the resulting rapidity distribution of net-baryons depends on the spatial form of the produced fireball. If the fireball is almost spherical, the expansion of the fireball is essentially 3-dimensional, which results in a peak at the midrapidity in the rapidity distribution. This statement is a theorem that can be proved in few lines. If a the fireball is strongly deformed (compressed) in the beam direction, *i.e.* it has the form of a disk, its expansion is approximately 1-dimensional that produces a dip at the midrapidity, which is confirmed by numerous simulations, see, *e.g.* [1]. In terms of the fluid mechanics this is a consequence of interaction of two rarefaction waves propagating from opposite peripheral sides of decaying disk toward its center [2].

The formation of this fireball is already a matter of dynamics at the early compression stage of the nuclear collision. The softest point [3] characteristic of EoSs with a phase transition plays an important role in this compression dynamics. At the softest point the system exhibits the weakest resistance to its compression as compared with that in adjacent regions of the EoS. At low collision energies the softest point is not reached in the collision process, the system remains stiff and therefore the produced fireball is almost spherical. As a result, the baryon rapidity distribution is peaked at the midrapidity. When the incident energy gets high enough, the softest-point region of the EoS starts to dominate during the compression stage, the system weaker resists to the compression and hence the resulting fireball becomes more deformed, *i.e.* more of the disk shape. Then its expansion is close to the 1-dimensional pattern and, as a result, we have a dip at the midrapidity. With energy rise, the stiffness of the EoS (in the range relevant to compression stage) grows, the system starts to be more resistant to the compression and hence the produced fireball becomes less deformed. The expansion of this fireball results in a peak or, at least, to a weaker dip at the midrapidity as compared to that at the "softest-point" incident energy. With further energy rise, the initial kinetic pressure overcomes the stiffness of the EoS and makes the produced fireball strongly deformed again, which in its turn, again, results in a dip at the midrapidity.

Thus, even without any nonequilibrium, we can expect a kind of a "peak-dip-peak-dip" irregularity in the incident energy dependence of the form of the net-proton rapidity

* Contribution to the Topical Issue "Exploring strongly interacting matter at high densities - NICA White Paper" edited by David Blaschke *et al.*

[a] e-mail: Y.Ivanov@gsi.de
[b] e-mail: blaschke@ift.uni.wroc.pl

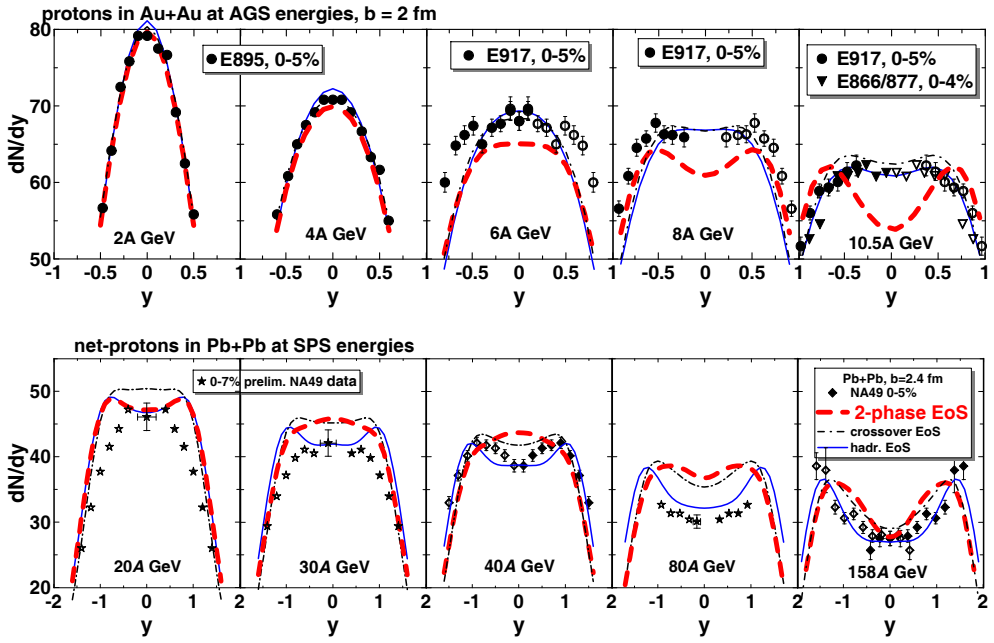

Fig. 1. Rapidity spectra of protons for AGS energies (upper-row panels) and net-protons SPS energies (lower-row panels) from central collisions of Au+Au (AGS) and Pb+Pb (SPS). Experimental data are from [17–22]. The percentage shows the fraction of the total reaction cross section, corresponding to experimental selection of central events.

distributions. Nonequilibrium also contributes to this irregularity. At a phase transformation the hadronic degrees of freedom are changed to partonic ones. In particular, the dip at the midrapidity in ultrarelativistic nuclear collisions occurs because the baryon charges of colliding nuclei traverse through each other rather than resulting from the 1-dimensional expansion of a disk-like fireball.

It is important to emphasize that the "peak-dip-peak-dip" irregularity is a signal from the hot and dense stage of the nuclear collision.

In the present paper this qualitative pattern is illustrated by calculations within a model of the three-fluid dynamics (3FD) [4] employing three different equations of state: a purely hadronic EoS [5] (hadr. EoS) and two versions of EoS involving deconfinement [6]: an EoS with the first-order phase transition (2-phase EoS) and that with a smooth crossover transition (crossover EoS). The softest points in these EoSs are illustrated in ref. [7]. The hadronic EOS [5] possesses no softest point, *i.e.* stiffness of the EoS changes monotonously. Results on the stopping power were reported in refs. [8–11] in more ditail.

2 Results of simulations

A direct measure of the baryon stopping is the net-baryon (*i.e.* baryons-minus-antibaryons) rapidity distribution. However, since experimental information on neutrons is unavailable, we have to rely on net-proton (*i.e.* proton-minus-antiproton) data. Presently there exist experimental data on proton (or net-proton) rapidity spectra at AGS [12–16] and SPS [17–22] energies.

Figure 1 presents calculated rapidity distributions of net-protons in central collisions at AGS and SPS energies and their comparison with available data. Difference between protons and net-protons is negligible at the AGS energies. As can be seen from fig. 1, the distributions within the first-order–taransition scenario indeed exhibit the above-discussed "peak-dip-peak-dip" irregularity in contrast to the results obtained within the purely hadronic and crossover scenarios. The experimental distributions exhibit a qualitatively similar behavior as that in the 2-phase EoS scenario. However, quantitatively the 2-phase EoS results certainly disagree with data in the energy region $8\,A\,\mathrm{GeV} \leq E_{\mathrm{lab}} \leq 40\,A\,\mathrm{GeV}$.

In order to quantify the above-discussed "peak-dip-peak-dip" irregularity, it is useful to make use of the method proposed in ref. [8]. For this purpose the data on the net-proton rapidity distributions are fitted by a simple formula:

$$\frac{\mathrm{d}N}{\mathrm{d}y} = a\left(\exp\left\{-(1/w_s)\cosh(y-y_s)\right\} + \exp\left\{-(1/w_s)\cosh(y+y_s)\right\}\right), \qquad (1)$$

where a, y_s and w_s are parameters of the fit. The form (1) is a sum of two thermal sources shifted by $\pm y_s$ from the midrapidity which is put to be $y_{\mathrm{mid}} = 0$, as it is in the collider mode. The width w_s of the sources can be interpreted as $w_s = (\mathrm{temperature})/(\mathrm{transverse\ mass})$, if we assume that collective velocities in the sources have no spread with respect to the source rapidities $\pm y_s$. The parameters of the two sources are identical (up to the sign of y_s) because only collisions of identical nuclei are considered. The above fit has been done by the least-squares method and applied to both available data and results of calculations.

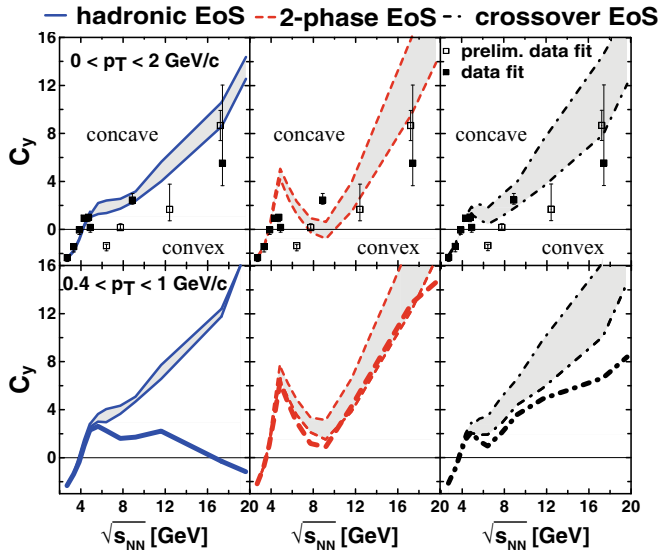

Fig. 2. Midrapidity reduced curvature (see. eq. (2)) of the (net-)proton rapidity spectrum as a function of the center-of-mass energy of colliding nuclei as deduced from experimental data and predicted by 3FD calculations with different EoSs: the hadronic EoS (hadr. EoS) [5] (left column of panels), the EoS involving a first-order phase transition (2-ph. EoS, middle column of panels) and the EoS with a crossover transition (crossover EoS, right column of panels) into the quark-gluon phase [6]. Upper bounds of the shaded areas correspond to fits confined in the region of $|y| < 0.7\, y_{\rm beam}$, lower bounds, $|y| < 0.5\, y_{\rm beam}$. Results are presented for two different windows of the transverse momentum p_T: $0 < p_T < 2\,{\rm GeV}/c$ (top-row panels) and $0.4 < p_T < 1\,{\rm GeV}/c$ (second-row panels). In the case of the $0.4 < p_T < 1\,{\rm GeV}/c$ window (second-row panels), results with additional constraint of $|y| < 0.5$ are displayed by corresponding bold lines.

A useful quantity, which characterizes the shape of the rapidity distribution, is a reduced curvature of the spectrum at midrapidity defined as follows:

$$C_y = \left(y_{\rm beam}^3 \frac{{\rm d}^3 N}{{\rm d}y^3}\right)_{y=0} \Bigg/ \left(y_{\rm beam} \frac{{\rm d}N}{{\rm d}y}\right)_{y=0} = (y_{\rm beam}/w_s)^2 \left(\sinh^2 y_s - w_s \cosh y_s\right), \qquad (2)$$

where $y_{\rm beam}$ is the beam rapidity in the collider mode. The second part of eq. (2) presents this curvature in terms of parameters of fit (1). Excitation functions of C_y deduced both from experimental data and from results of the 3FD calculations with different EoSs are displayed in fig. 2. To evaluate errors of C_y values deduced from data, errors produced by the least-squares method were estimated. The uncertainty associated with the choice of the rapidity range turned out to be the dominant one for the C_y quantities deduced from simulation results. Therefore, in fig. 2, results for the curvature C_y in the wide rapidity range are presented by shaded areas with borders corresponding to the fit ranges $|y| < 0.7\, y_{\rm beam}$ and $|y| < 0.5\, y_{\rm beam}$.

The irregularity in the data is distinctly seen here as a wiggle irregularity in the energy dependence of C_y. Of course, this is only a hint to irregularity since this wiggle is formed only due to preliminary data of the NA49 Collaboration. A remarkable observation is that the C_y excitation function in the first-order–transition scenario manifests qualitatively the same wiggle irregularity (middle upper panel of fig. 2) as that in the data fit, while the hadronic scenario produces purely monotonous behavior. The crossover EoS represents a very smooth transition, therefore, it is not surprising that it produces only a weak wiggle in C_y.

3 Effect of the experimental acceptance

The above calculations were performed assuming the acceptance for net-protons to be wide enough to include almost all emitted particles. In practice, the extension of the acceptance beyond the range of $0 < p_T < 2\,{\rm GeV}/c$ does not practically change the net-proton rapidity distributions in the incident-energy range of interest. However, the actual experimental acceptance can be narrower. For the NICA MPD experiment it is restricted by the proton identification capabilities in the TOF detector to $0.4\,{\rm GeV}/c < p_T < 1.0\,{\rm GeV}/c$ in the central rapidity range $|y| < 0.5$ [23]. Calculations performed for the NICA-MPD acceptance [24] are presented in the lower-row panels of fig. 2.

The application of the p_T cut without confining the rapidity range (shaded bands in lower-row panels of fig. 2) does not qualitatively change the picture. As can be seen from fig. 2, the wiggle in the energy dependence of C_y is a very robust signal of the first-order phase transition. It survives even at this limited p_T-acceptance. The important difference between different p_T-acceptances is that the wiggle is completely located in the range of positive curvatures C_y (concave shapes of the rapidity distribution near midrapidity). Therefore, the name of "peak-dip-peak-dip" for this irregularity becomes not quite correct. The crossover scenario results in a very weak wiggle in C_y.

The actual MPD acceptance conditions also include the restriction $|y| < 0.5$. Applying this restriction in addition to the p_T cut leads to the corresponding bold lines in fig. 2. As can be seen from fig. 2, under the constraints of the MPD acceptance conditions the wiggle in the energy dependence of C_y is very robust for the first-order phase transition and the crossover one. However, this is not the case for the hadronic EoS. The hadronic-EoS C_y excitation functions now exhibit a local weak wiggle in the region $5 < \sqrt{s_{NN}} < 12\,{\rm GeV}$ qualitatively similar to that for the crossover transition. Moreover, the C_y curvature becomes negative at $\sqrt{s_{NN}} = 19.6\,{\rm GeV}$ that contradicts natural expectations that the net-proton distribution at midrapidity proceeds from convex shape (strong stopping) to a concave one (an increasing transparancy) with the beam energy rise. These peculiarities are a consequence of a fine structure of the rapidity distribution near midrapidity that becomes dominant in the narrow rapidity window $|y| < 0.5$. This situation is illustrated in fig. 3. It is seen

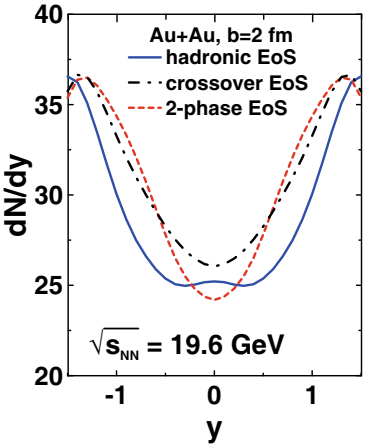

Fig. 3. Rapidity distribution of net-protons in central ($b = 2\,\mathrm{fm}$) Au+Au collisions at collision energy $\sqrt{s_{NN}} = 19.6\,\mathrm{GeV}$ for the case of the p_T range $0 < p_T < 2\,\mathrm{GeV}/c$.

that, at $\sqrt{s_{NN}} = 19.6\,\mathrm{GeV}$, there is a tiny maximum at the midrapidity in the hadronic-EoS rapidity distribution, which results in the negative curvature observed in fig. 2. The analysis of the net-proton distributions in the narrow rapidity window reveals only a fine structure of the rapidity distribution near midrapidity, which could be just an artifact of a simplified treatment of the complicated nonequilibrium stage of the collision based on the three-fluid approximation. In order to conclude on the baryon stopping we need to analyze the global shape of the rapidity distributions. The global shape of the hadronic-EoS rapidity distributions does not exhibit such peculiarities, as is clear from C_y calculations in a wider rapidity range.

Therefore, we can conclude that under the conditions of the MPD acceptance it is possible to distinguish the first-order phase transition, the onset of which is signalled by a strong wiggle in the excitation function of C_y. However, the difference between the purely hadronic case and that with the smooth crossover transition becomes ambiguous.

4 Conclusions

In conclusion, the irregularity in the baryon stopping is a natural consequence of the deconfinement occurring at the compression stage of a nuclear collision and thus is a signal from the hot and dense stage of the nuclear collision. It is an effect of the softest point of a EoS. It was demonstrated that this irregularity is a very robust signal of a first-order phase transition that survives even under conditions of a very limited acceptance [24]. Updated experimental results are badly needed to analyze a trend of the "peak-dip-peak-dip" irregularity. It would be highly desirable if new data are taken within the same experimental setup.

We are grateful to A.S. Khvorostukhin, V.V. Skokov, and V.D. Toneev for providing us with the tabulated 2-phase and crossover EoSs. Our thanks go to O. Rogachevsky and V. Voronyuk for information about the acceptance range of the TOF detector in the NICA MPD experiment. The calculations were performed at the computer cluster of GSI (Darmstadt). The work of DB was supported in part by the Polish NCN under grant UMO-2011/02/A/ST2/00306 and by the Hessian LOEWE initiative through HIC for FAIR.

References

1. V.N. Russkikh, Yu.B. Ivanov, Phys. Rev. C **76**, 054907 (2007).
2. L.D. Landau, E.M. Lifshitz, *Fluid Mechanics* (Pergamon Press, Oxford, 1979).
3. C.M. Hung, E.V. Shuryak, Phys. Rev. Lett. **75**, 4003 (1995).
4. Yu.B. Ivanov, V.N. Russkikh, V.D. Toneev, Phys. Rev. C **73**, 044904 (2006).
5. V.M. Galitsky, I.N. Mishustin, Sov. J. Nucl. Phys. **29**, 181 (1979).
6. A.S. Khvorostukhin, V.V. Skokov, K. Redlich, V.D. Toneev, Eur. Phys. J. C **48**, 531 (2006).
7. E.G. Nikonov, A.A. Shanenko, V.D. Toneev, Heavy Ion Phys. **8**, 89 (1998).
8. Yu.B. Ivanov, Phys. Lett. B **690**, 358 (2010).
9. Yu.B. Ivanov, Phys. At. Nucl. **75**, 621 (2012).
10. Yu.B. Ivanov, Phys. Lett. B **721**, 123 (2013).
11. Yu.B. Ivanov, Phys. Rev. C **87**, 064904 (2013).
12. E-0895 Collaboration (J.L. Klay *et al.*), Phys. Rev. C **68**, 054905 (2003).
13. E802 Collaboration (L. Ahle *et al.*), Phys. Rev. C **60**, 064901 (1999).
14. E877 Collaboration (J. Barrette *et al.*), Phys. Rev. C **62**, 024901 (2000).
15. E917 Collaboration (B.B. Back *et al.*), Phys. Rev. Lett. **86**, 1970 (2001).
16. J. Stachel, Nucl. Phys. A **654**, 119c (1999).
17. NA49 Collaboration (H. Appelshäuser *et al.*), Phys. Rev. Lett. **82**, 2471 (1999).
18. NA49 Collaboration (T. Anticic *et al.*), Phys. Rev. C **69**, 024902 (2004).
19. NA49 Collaboration (C. Alt *et al.*), Phys. Rev. C **73**, 044910 (2006).
20. NA49 Collaboration (C. Blume), J. Phys. G **34**, S951 (2007).
21. NA49 Collaboration (T. Anticic *et al.*), Phys. Rev. C **83**, 014901 (2011).
22. NA49 Collaboration (C. Alt *et al.*), Phys. Rev. C **68**, 034903 (2003).
23. S.P. Merz, S.V. Rasin, O.V. Rogachevsky, talk given at the Russian Academy of Sciences (2012) `http://mpd.jinr.ru/data/presentations/ras/merts.pdf`.
24. Y.B. Ivanov, D. Blaschke, Phys. Rev. C **92**, 024916 (2015).